Fitting QSO Spectra

The purpose of this document is to provide additional information on the process of fitting optical AGN spectra as described in the paper 'Behaviour of the MgII 2798Å Line Over the Full Range of AGN Variability' (*link*). The scripts used to create the samples and do the fitting are provided in this GitHub link. This allows interested readers of the paper to inspect the methods of analysis used to produce fits and the data presented in the figures and tables. In the following we will first provide a brief overview of the contents and purpose of the different Python files, followed by a more in-depth discussion of the fitting algorithm.

1 Guide to the Accompanying Python Scripts

A basic description of the classes and functions defined in these scripts is provided in their docstrings, however we provide an overview of the different Python files below.

1. Spectrum: The class definition of 'Spectrum' which contains methods for fitting optical spectra. The methods are built on the `lmfit` package[1].

2. Norm_and_Fit: The class definitions of 'Normalisation' and 'Fit'. 'Normalisation' contains the methods to create the normalised data files used for further analysis. The normalisation is in accordance with the definitions laid out in the paper. The 'Fit' class provides methods for analysis and contains the method (create_figure) for making the majority of the figures in the paper.

3. fp_define: This script lays out the selection process for the Full Population sample.

4. fp_fit_spectra: The implementation of the fitting algorithm for the Full Population sample, following the procedure presented in the paper and discussed in more detail below.

5. fp_figures: Examples of use for the 'Normalisation' and 'Fit' methods. The comments in the documents indicate which methods were used to create which figures.

6. sv_figures: As 'fp_figures', but for Supervariable sample.

2 Overview of the Fitting Process

The outline of the fitting process is presented in section 3 of the paper. Taking a closer look at the individual stages: (1) When the spectrum is loaded, the bins without an error associated with the flux measurement are masked out. (2) Deredden the spectra, correcting for Galactic extinction. This extinction is due to dust in the Milky Way, along the line of sight to the target. The flux loss due to this interaction affects the blue side of the spectrum more than the red. As it is possible to make use of multiple empirical extinction curves to correct for this effect, it is worthwhile to briefly discuss the choice made for the pipeline. The dereddening curve applied to the spectra here is that described in Fitzpatrick (1999) (F99). The implementation of the F99 correction is with a function from the python `extinction` package[2]. The choice of function is in accordance with the analysis of Schlafly & Finkbeiner (2011) (S&F), who compare the extinction models of F99 and Cardelli et al. (1989) (CCM), using SDSS stellar spectra.

The values of A_V for the objects in the sample are downloaded from the NASA/IPAC IRSA website[3], which uses a map of galactic dust (Schlegel et al., 1998) to estimate the dust temperature and column density. The coordinates used for the objects are from DR7Q. The selected extinction measure is that based on the model of S&F, and the `extinction` function dereddens the spectrum according to the E(B-V) values set in F99.

Following the extinction correction, (3) the spectrum is trimmed to the wavelength range for the initial fitting process. The different spectral components are fit in different wavelength windows. An overview of the relevant ranges is given in table 1. The spectrum is not deredshifted yet. Rather, the spectral components are redshifted into the QSO restframe, such that z is also estimated in the fit. The application of the windows is followed by (4) calling the fitting algorithm. The algorithm consists of the

[1] https://lmfit.github.io/lmfit-py/
[2] https://extinction.readthedocs.io
[3] https://irsa.ipac.caltech.edu/applications/DUST/

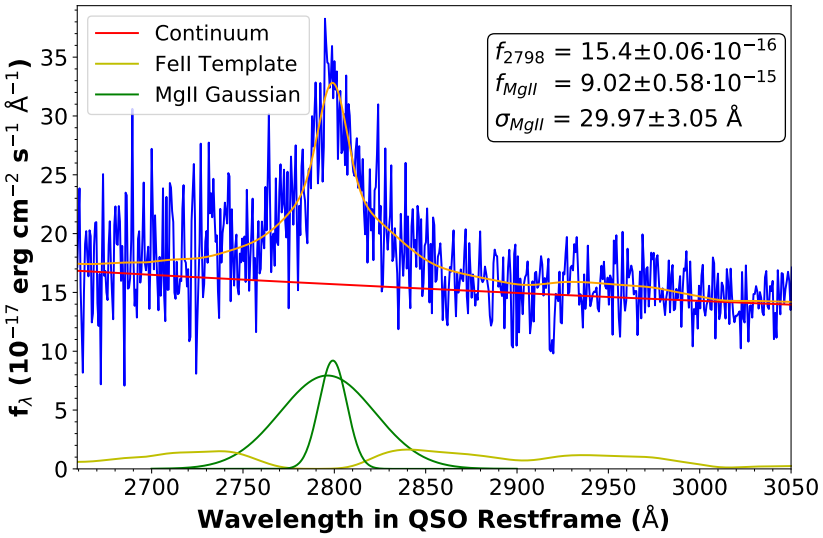

Figure 1: Example of the result of a fit by the pipeline, for the SDSS spectrum of J212436 taken on MJD 52200. The spectrum is shown in blue and the fit components are: *red*: power law continuum; *green*: Gaussian fit to MgII (this can be one or two Gaussians); *yellow*: FeII template by Vestergaard et al., smoothed with a Gaussian filter; *orange*: the combined fit to the spectrum. Note in particular the presence of FeII emission in both the red and the blue wing of the MgII line.

methods provided by the `lmfit` package. The results of the fit are then (5) used in the next iteration of the fit, both in a sigma-clipping of the data and as initial estimates for the function parameters.

2.1 Spectral Components and Iterative Fitting

The components of the model used to fit the MgII line are the continuum power law, the FeII template, and one or two Gaussian profiles for the MgII line itself. Each component is fit iteratively, with the initial guesses for the model parameters, used as the starting point for the χ^2 minimisation algorithm, set to the same value for every spectrum. The number of iterations and the sigma-clipping limit are free parameters in the procedure, for every spectral component. The pipeline was calibrated to the Supervariable sample, which includes both SDSS and new spectra, before being applied to the much larger Full Population sample. An overview of the parameters used in the pipeline is displayed in table 1. An example of a spectral fit, with all components identified, is shown in figure 1.

The power law continuum is defined as $A\nu^{-\alpha}$, where A is the amplitude and α the power law index. This is the first component to be fitted. The wavelength range is selected to contain as few contaminating features in the spectrum as possible, and to provide a good representation of the continuum in the near-UV. This step is only repeated once: after the initial fit has been completed, the pipeline calculates the standard deviation of the residuals, and then removes all data points that are further than 2 standard deviation away from this fit (sigma clipping). The fit is then repeated on the clipped data-set with the results of the previous fit as the initial estimate for the model parameters.

One of the main benefits of iterative fitting is that it circumvents a recurring issue with the `lmfit` algorithm, in which it cannot return errors on a fit with noisy data. By reducing the required exploration of the parameter space (using the new initial values) and reducing the noise in the data, it is possible to get a better estimate of the uncertainties involved in the fitting procedures. The errors returned in the basic `lmfit` functionality are the standard errors calculated from the covariance matrix. As discussed further the paper (section 3) these fitting errors are almost certainly an underestimate of the model uncertainties, and will be superseded by other estimates. However, for their use in the calculation of the reduced χ^2 and in the choice of the correct FeII template it was important to have these `lmfit` estimates available.

Following the power-law-only fit, the same spectral range is used to jointly fit the power law and the FeII template. The FeII template used in this step is that presented by Vestergaard & Wilkes (2001) (see the discussion in section 2.2 for further details). The pipeline starts with the original data, but uses the results from the power law fit as the initial parameter values for this component. The FeII component of

the model has three parameters: the amplitude, representing the strength of iron emission, the redshift, fixing the position of the lines, and a smoothing parameter. The smoothing parameter is defined as the width of the Gaussian kernel that is used in the smoothing process. The physical interpretation of this smoothing is kinematic broadening of the iron lines: at least part of the FeII emission is expected to come from relatively deep in the potential well. The effect of this broadening on the template is to blend the many lines together, smoothing the overall profile. The fitting is repeated four times, with the same value for the sigma-clipping as for the power-law-only case. After the final iteration, the best fit continuum+FeII model is subtracted from the full data-set.

The final component of the fit is the line itself, which is calculated in the window $2700 < \lambda < 2900$Å using the residuals derived in the previous step. The line is represented with one or two Gaussian profiles. Although most spectra are best approximated with a single Gaussian, there are examples (such as in figure 1) where there is a clear second component, and two Gaussians are needed to best capture the line flux. The selection between the two models is left to the algorithm, and is based on the Akaike Information Criterion (AIC). For the MgII line, both the single and double Gaussian model are fit to the data. The fitting procedure is the same for each: three iterations, with data being clipped when it is further than three σ away from the model. After this fitting, the AIC is calculated for both models, and the model with the lowest AIC is selected. Note that the second Gaussian, although narrower than the other component, does not constitute a 'narrow' line in the same sense as e.g. the [OIII] narrow lines. It is assumed that the true narrow component of MgII, in as far as it is present, is not resolved. In the case where two Gaussians are fit, their combined flux constitutes the broad MgII emission.

2.2 Selecting the FeII Template

The presence of significant FeII emission in the wings of the MgIIλ2798 line means the choice of FeII template and the subsequent fitting are a source of possible uncertainty in the analysis. There are several FeII emission templates available, and different templates for different parts of the spectrum. To optimise the fitting process, it important to select the template that provides the most consistent measurement of the MgII flux. We have tested two UV FeII templates: the empirical template presented in Vestergaard & Wilkes (2001) (VW) and the template based on an FeII transition model presented in Bruhweiler & Verner (2008) (BV). The VW template is the template used in DR7Q for the MgII region.

The VW template is based on spectra from the narrow line Seyfert 1 galaxy I Zw 1, which has unusually strong iron emission lines. In applying this template to other AGN, the relative strength of the different emission lines found in I Zw 1 is therefore assumed to be universal, with only the overall amplitude varying in the fit. The BV template is based on a model of the FeII atom, covering 830 possible energy levels, and the associated transitions. This model was combined with the CLOUDY software (Ferland et al., 2013) to produce a synthetic FeII emission spectrum, which was also calibrated to I Zw 1. Although calibrated to the same object there are significant differences between the two templates, especially for the emission in the wings of MgII. Whereas the VW template has more or less symmetric bumps on either side, the BW template has significantly stronger emission on the blue side of the line.

The comparison of the templates' applicability was made by fitting the models containing the two different templates to the same spectrum and comparing the errors. The other components of the model are the power law and only a single Gaussian. To account for a possible underestimation of the errors by `lmfit`, an error measure was calculated using a simple Monte Carlo simulation. For N=10^3 iterations Gaussian noise was added to the flux data, where the spread in the noise was chosen to be the measurement error on the flux. As described in the paper, two main quantities under consideration for the study are the MgII line flux and the estimated continuum flux at 2798Å. For each of the 10^3 spectral fits these quantities are calculated. The spread in their distribution (the standard deviation σ_{MC}) is used as an error measure on the two model fits. The spectrum used for the fitting was the SDSS spectrum for J002714, an object in the supervariable sample. The model fitting followed the same procedure as outlined in section 2.1.

The results of the comparison suggest a slight preference for the VW template. For VW $\sigma_{MC,line} = 3.19 \cdot 10^{-15}$ erg s^{-1} cm^{-2} and $\sigma_{MC,continuum} = 2.74 \cdot 10^{-17}$ Å^{-1} erg s^{-1} cm^{-2}. For the BV template the error measures are: $\sigma_{MC,line} = 3.19 \cdot 10^{-15}$ erg s^{-1} cm^{-2} and $\sigma_{MC,continuum} = 4.22 \cdot 10^{-17}$ Å^{-1} erg s^{-1} cm^{-2}. As an additional check, I compared the reduced χ^2 for the two fits. The ratio of $\chi^2_{red,VW}$ to $\chi^2_{red,BV}$ is approximately 0.92, again indicating a preference for the VW template. Inspection by eye did not suggest a strong favourite for either of the two templates. The VW template was selected for use in the pipeline, as this statistical comparison indicates it works better with the applied fitting procedure.

Table 1: The components of the spectral fitting model for the MgII pipeline, and the parameters used for the fitting process. The columns, from left to right, are the name of the component, the wavelength window in which the component is fit, the number of iterations used in the pipeline in fitting the component, the number of standard deviations used as a measure to smooth the data after each iteration of the fit (σ-clipping), the parameters used to fit the model component, and finally the initial values for each parameter in `lmfit`, used in the first iteration of the fit.

Spectral Component	λ range (QSO restframe)	N_{iter}	σ_{clip}	Parameters	Initial value
Continuum	$2300 < \lambda < 2700$ $2900 < \lambda < 3088$	2	2	Amplitude Index	10^{-17} erg Å^{-1} s^{-1} cm^{-2} -1
FeII	$2300 < \lambda < 2700$ $2900 < \lambda < 3088$	4	2	Amplitude z Smoothing par.	10^{-15} erg s^{-1} cm^{-2} z from DR14Q 5 (min= 0)
MgII (Gaussian)	$2700 < \lambda < 2900$	3	3	Amplitude width centre	$5 \cdot 10^{-15}$ erg s^{-1} cm^{-2} 40 Å (max= 100 Å) $2798 \cdot (1+z)$ Å
MgII (two Gaussians)	$2700 < \lambda < 2900$	3	3	1) Amplitude 1) width 1) centre 2) Amplitude 2) width 2) centre	$2 \cdot 10^{-15}$ erg s^{-1} cm^{-2} (min= 0) 10 Å (max= 25 Å) $2798 \cdot (1+z)$ Å $7 \cdot 10^{-15}$ erg s^{-1} cm^{-2} (min= 0) 40 Å (min= 0, max= 65 Å) $2798 \cdot (1+z)$ Å

References

Bruhweiler F., Verner E., 2008, ApJ, 675, 83
Cardelli J. A., Clayton G. C., Mathis J. S., 1989, ApJ, 345, 245
Ferland G. J., et al., 2013, Rev. Mex. Astron. Astrofis., 49, 137
Fitzpatrick E. L., 1999, PASP, 111, 63
Schlafly E. F., Finkbeiner D. P., 2011, The Astrophysical Journal, 737, 103
Schlegel D. J., Finkbeiner D. P., Davis M., 1998, ApJ, 500, 525
Vestergaard M., Wilkes B. J., 2001, the Astrophysical Journal Supplement, 134, 1